A Hybrid Approach to Motion Prediction for Ship Docking—Integration of a Neural Network Model Into the Ship Dynamic Model

Robert Skulstad[ID], Guoyuan Li[ID], *Senior Member, IEEE*, Thor I. Fossen[ID], *Fellow, IEEE*, Bjørnar Vik[ID], and Houxiang Zhang[ID], *Senior Member, IEEE*

Abstract—While automatic controllers are frequently used during transit operations and low-speed maneuvering of ships, ship operators typically perform docking maneuvers. This task is more or less challenging depending on factors, such as local environment disturbances, the number of nearby vessels, and the speed of the ship as it docks. This article proposes a tool for onboard support that offers position predictions based on an integration of a supervised machine learning (ML) model of the ship into the ship dynamic model. The ML model is applied as a compensator of the unmodeled behavior or inaccuracies from the dynamic model. The dynamic model increases the amount of predetermined knowledge about how the vessel is likely to move and, thus, reduces the black-box factor typically experienced in purely data-driven predictors. A prediction horizon of 30 s ahead of real time during docking operations is examined. History data from the 29-m coastal displacement ship Research Vessel (RV) Gunnerus are applied to validate the approach. Results show that the inclusion of the data-based ML model significantly improves the prediction accuracy.

Index Terms—Onboard support, ship motion prediction, supervised deep learning.

I. INTRODUCTION

SHIP motion prediction is a general term that incorporates many elements. These include the states to perform predictions—for example, prediction of ship orientation, position, or up/down motion—the temporal aspect (long, medium, and short) and the model that makes the prediction of the states in the near future. Typically, these predictions, which are based on time-series data, coincide with a specific application that could benefit from having information about future states of the vessel motion. Historically, research efforts have been focused on ship orientation and applications where safety or efficiency can be increased using predictions of these states. Mainly, this is due to the abundance of operations that are severely impacted by angular motions of a vessel, including takeoff and landing of autonomous aerial vehicles and helicopters [1], crane operations [2], [3], and missile launch [4]. These operations can be made safer and more efficient by incorporating knowledge about future vessel states.

Docking is the task of maneuvering the vessel to a fixed mooring location. On the path toward the dock, the vessel operator must tackle challenges such as passing/nearby vessels, compensating for forces induced on the vessel by environment disturbances, and arriving at the dock location in a timely fashion. The latter is especially important for ferries or vessels transporting goods on a fixed route, where keeping the time schedule is key. Although much effort has been put into ship autonomy in recent years [5], docking is still a largely manual task performed by the vessel operator. Research in the field of ship motion prediction typically focuses on methods within one domain, e.g., dynamic or kinematic models and Kalman filters (KFs), machine learning (ML), and deep learning or autoregressive (AR) methods (see Section II).

Dynamic models aim at describing the motion of the vessel due to forces estimated by simplified representations of the vessel, including thruster effects and, to some extent, forces due to environmental disturbances. Simplifications are necessary due to the lack of direct measurements of wave/current drift. In addition, for docking applications, effects due to local wind fields, cushioning effects at the dock, and shallow water exist, which are not measured directly. The true model is complex and nonlinear; thus, a simplified model is often used, and the discrepancies between the behavior of the real ship and the dynamic model are expected. Kinematic prediction models allow for translating motion measurements, such as accelerations, into predictions of position. However, they account for neither the effects of thruster commands nor the direct effect of wind forces. While many ML methods are well suited for representing nonlinear models, they require a substantial amount of sampled data to do so reliably. In addition, the inner connections in an ML model may not be readily understandable.
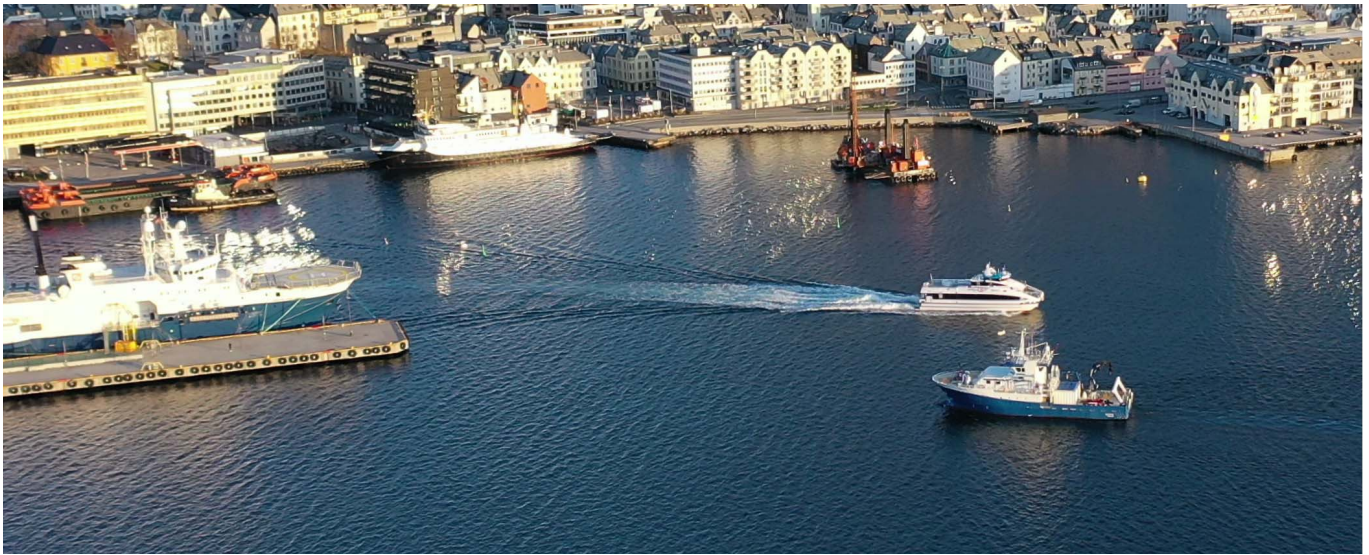
Fig. 1. RV Gunnerus of the NTNU (bottom right vessel) approaching a dock in the port of Ålesund, Norway.

Examples where existing knowledge of the behavior of the ship is utilized in cooperation with data-based ML models are scarce. This study will, therefore, investigate the feasibility of one such approach: making position predictions using a dynamic model, while, in parallel, an ML model predicts the position prediction error made by the dynamic model in order to compensate for any unmodelled behavior or inaccuracies. Including the measured wind velocity and direction as input to the ML model contributes significantly to the success of the proposed approach. While a KF could simulate the dynamic model and derive predictions in a similar manner, the ability to provide corrections to the dynamic model predictions, gained by learning from docking examples differing in port location, sea state, and wind conditions, would be lost. This work will focus on the prediction of position during the docking operation of a regular displacement ship. Fig. 1 shows a picture of the ship. Currently, this is a manual task, relying on the ship operator to make appropriate and timely corrections to actuators in order to safely dock the vessel. During this operation, the ship operator must make many choices due to changing environmental factors, regulations calling for proper interaction with nearby/crossing vessels, and the effects of applied actuator commands. To aid in making these choices, this article proposes an onboard support tool, which will provide the vessel operator with predictions of the vessel position. These predictions originate from the hybrid predictor and span 30 s into the future [6], hereafter termed the prediction horizon. Key contributions of this article include the construction of a hybrid model for prediction of the future motion of a ship and the use of data sampled onboard a coastal ship for the training of the data-based model, as well as verification of the prediction performance.

The remainder of this article is organized as follows. Section II presents previous research in this domain. Section III introduces the predictors and their architecture/parameters. Section IV gives results and describes the vessel and data selected for training and testing of the predictors. Section V presents the conclusions.

II. RELATED WORK

Research on ship motion prediction generally revolves around a model that processes time-series data, where each input channel contains data sampled at a fixed time interval. Several metrics exist in which time-series prediction models may be categorized. If the model uses existing explicit knowledge of how the vessel moves due to forces and/or velocities (dynamic/kinematic models), the term model-based predictors may be appropriate. If only sampled data are used to learn the behavior of the vessel, the predictor is termed data-based. We may also distinguish methods based on whether they can represent nonlinear behavior. The following subsections outline the description and classification of existing methods for ship motion prediction.

A. Model-Based Motion Prediction

This section introduces predictors applying predetermined knowledge of how the vessel behaves when maneuvering.

1) Dynamic Model: Triantafyllou *et al.* [7] used a standard KF to estimate and predict the motion states of the two decoupled motion groups heave–pitch and roll–sway–yaw. They found that in order for the KF to be successful, an accurate model of both vessel and sea state spectrum was required. For the latter requirement, the estimation of the modal frequency of the spectrum was key to the performance of the KF.

Sutulo *et al.* [8] aimed at creating maneuvering models (dynamic or kinematic) that could be inexpensive to evaluate and, thus, be used in tasks related to prediction and onboard support. According to the authors, this could make applications, such as model-based collision avoidance and onboard decision support for deciding control commands feasible due to the computational efficiency of the models.

2) Motion Density Functions: Instead of using the equations of motions to model the dynamic behavior of vessel states, as Triantafyllou *et al.* [7] had done, Sidar and Doolin [9] constructed the linear KF using approximations of density functions of measured heave and pitch motions. The density functions were obtained experimentally. This led to a KF of significantly lower dimensions compared with the work of Triantafyllou *et al.* [7]. Measured heave and pitch time series were assumed to be stationary, narrow band, and stochastic for the duration of the prediction interval. The choice of a KF as a tool for making predictions using the motion density functions was motivated by its ability to produce predictions in real time.

The approach to ship motion prediction taken by Nielsen *et al.* [10] also relies on density functions of time-series data. By deriving the observed autocorrelation matrix for variables largely dictated by the induced wave force, predictions of 15–60 s were made on a model-scale ship.

3) Kinematic Model: Perera and Guedes Soares [11] and Perera *et al.* [12] proposed to use the extended KF (EKF) to estimate the translational motion states and predict the trajectory of a vessel by means of a curvilinear motion model (CMM). States included in this model were heading angle, normal and tangential accelerations, forward (surge) speed, and sideways (sway) speed. By combining the EKF and the CMM, the authors found that the estimated velocities and accelerations, which were estimated based only on noisy position measurements, converged quickly (within 15 s) to small variations around the true values. For the validity of the prediction, they assumed constant accelerations, which is a strong assumption, given the nature of vessel motion. This was acknowledged by the authors, deeming the approach valid only for short-term predictions.

Perera [6] later modified his approach to using a vector dot and cross product algorithm for the prediction of vessel motion. Given the large inertia of a vessel, its trajectory creates a curve in the ocean plane, motivating the use of the CMM as a vessel model in the EKF. Based on this property, the algorithm calculates the radii of the center of gravity and pivot point of the vessel relative to a calculated center of planar motion for a vessel. The states and parameters related to the vessel pivot point were estimated for a given time instance and used to predict the position and heading 30 s ahead of real time. The adaptability to varying conditions is, according to the author, preserved by the use of the EKF, and predictions are valid under the assumption of constant navigation conditions within a short future time interval.

B. Data-Based Motion Prediction

To address the difficulty of obtaining a sufficiently detailed mathematical model, which transitions the relevant states from one sampling time instance to the next, many researchers have turned to data-based predictor models. The principal advantage of such methods is the ability to construct a model that relates a certain sampled input vector to a certain output state vector without knowledge of the parameters of the physical object. This output state vector is a set of vessel states for which one wishes to determine numerical values ahead of real time. Support vector machines (SVMs), neural networks, and AR models are examples of such methods, and the majority of data-based predictor models used for ship motion prediction are varieties of these general models.

SVM features attributes such as strong generalization ability and global optimization [13]. Creating a model that is able to generalize well to inputs, beyond those provided in the learning stage of the method, is one of the key advantages of this method. Li *et al.* [14] used SVM, together with several aiding methods, to predict the heave motion, given waves impacting the vessel at four different directions.

The attributes of neural networks include the ability to adapt to input changes and represent the nonlinear behavior of the input–output relation of physical systems. Employing a time-delay neural network with wavelet activation functions and using sensitivity analysis to determine significant inputs, Zhang and Liu [15] performed prediction of the heading of a vessel a few steps ahead. They concluded that this type of prediction may be used for the benefit of vessel control and safety.

Peng *et al.* [16] applied data-based modeling to estimate the unknown ship dynamics, as well as to reconstruct the unmeasured ship velocity. An echo state network [16] and a fuzzy system [17] comprise the tools that were integrated into an observer and subsequently used in vessel maneuvering control. The task of reconstructing the entire dynamic model of the vessel was relaxed through the introduction of a nominal mass matrix in [16]. Force produced by thrusters on the vessel was assumed to be known and subsequently input to the data-based model to approximate the vessel dynamics.

Yin *et al.* [18] used a single-layer feedforward network (SLFN) to predict the heading angle of a vessel a few sample intervals ahead. This one-layer prediction network is common in the literature although the choice of activation function, training method, number of hidden neurons, type and number of input variables, and the number of input lags vary greatly. Arriving at suitable values for these parameters is the key challenge to providing reliable predictions using SLFNs. Often these parameters are derived using trial and error although online pruning methods for producing compact networks exist [19]. For statically trained networks, genetic algorithms, grid search, or random search algorithms may also be used to optimize architecture and hyperparameters.

Skulstad *et al.* [20] applied a long short-term memory (LSTM) network, a version of a recursive network, to maintain estimates of position and heading of a ship during the loss of position reference signals from the global navigation satellite system. They used a deep neural network similar to the one described in Section III-C. However, only a one-step prediction was made, and the sensors that are not relying on external signals, such as the compass, wind sensor, and sensors measuring operating conditions of the thrusters, were still active.

Maintaining accurate estimates of position and attitude during the loss of GNSS signals is also of importance in the automotive and aerospace domains. Examples of approaches to mitigate such a sensor loss, through one-step predictions,
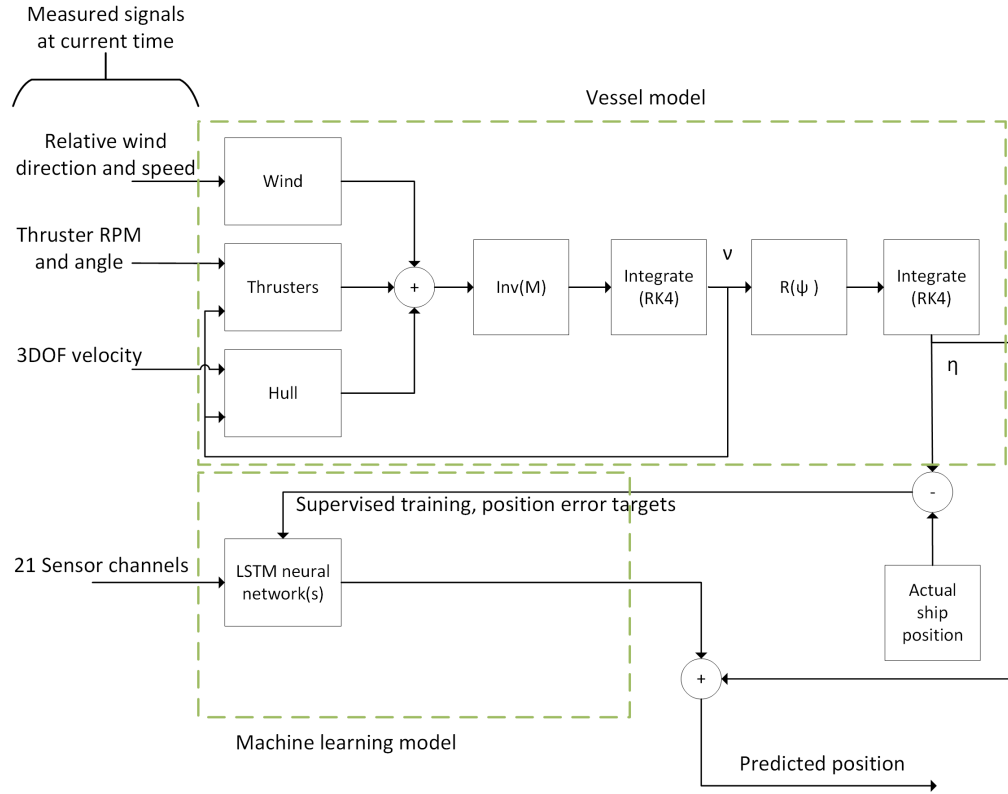
Fig. 2. Prediction strategy showing the vessel model predictor (upper dashed rectangle) and the ML model (lower dashed rectangle).

are given in [21] and [22]. The former applies a KF in combination with an AR integrated moving average model and a feedforward neural network to predict errors accumulating in the inertial navigation system, while the latter makes use of a radial basis function neural network for predicting the KF measurement update.

The AR method makes use of history samples of the target state accompanied by predictor model parameters determined by a least-squares method [23]. It offers low computational costs but has drawbacks handling nonlinear, nonstationary series [24]. Derivative methods to mitigate the effects of these drawbacks exist, such as nonlinear AR method and time-varying AR method. To predict the displacement of a landing deck on a vessel, Yang [1] improved upon the standard AR method by using Bayes information criterion to determine the number of model coefficients and a forgetting factor to reduce the effect of older vessel states on the regression algorithm output.

Lately, studies on vessel traffic management have resulted in more emphasis on trajectory prediction in order to improve operational safety in congested waters [12], [25], [26]. However, these are long-term predictions and fall outside the scope of this work. Similarly, the prediction of a maximum envelope of the roll, pitch, or heave motion, termed quiescent period prediction (see [27], [28]) is out of scope for this study.

Prediction using time-series methods similar to the ones described earlier is also found in various other domains, such as weather prediction [29], electrical load forecasting [30], and automotive motion prediction [31].

III. PREDICTOR MODELING

As the proposed method in this study is a combination of two predictor models originating from two separate fields, model-based and data-based, the following will outline how they are constructed and how they cooperate to predict the future ship motion.

A. Hybrid Predictor

In order to utilize the two complementary predictors for creating a hybrid predictor, the vessel model predictor (see Section III-B) will act as a foundation, predicting the complete position state due to the sampled data it receives. As the relative water velocity is not measured onboard the vessel nor are the effects of the waves on the vessel motion directly accounted for, a certain disagreement between the actual motion of the vessel and the position prediction output by the vessel model is expected. To compensate for the prediction errors made by the vessel model, the ML model is applied (see Section III-C). In this way, the hybrid prediction is the sum of the prediction made by the vessel model and the ML model. Fig. 2 shows how the two models are combined to create a predictor of the future ship position. The top dashed box of Fig. 2 shows the individual components of the vessel model (see Section III-B for a detailed description).

A fundamental difference between the vessel model and the ML model is the way they produce prediction output. While the ML model directly outputs predictions for the entire prediction horizon (for future times $t_h = [1–30]$ s), the vessel

model requires iterations. Thus, during the training of the hybrid predictor, for each time instance in the input data, the vessel model is iterated 30 times in order to produce targets for supervised training. This is illustrated by the block named actual ship position and the subtraction of the position, η, predicted by the vessel model. During this iterative process, external signals such as thruster RPM and angle, wind speed and angle, and measured velocities are not updated as they are not known for future time instances. However, feedback loops are present inside the vessel model, causing dynamic behavior within the prediction horizon in terms of thruster forces and vessel velocities. Training the ML predictor involves using the position error targets and the associated input vector to get optimized hyperparameters that reflect the dynamics of the error model (see Section III-C). As there are no feedback loops between the targets and the input vector of the ML supervised learning approach, it is termed open-loop. The description of the variables included in the input vector may be found in Table II. The bottom dashed box of Fig. 2 is repeated, applying identical hyperparameter values, so as to create an ensemble of LSTM predictors (more details on this are given in Section III-C1). To get hybrid position predictions during a docking operation, the sum of the vessel model position prediction η and the LSTM model error prediction is calculated.

B. Vessel Model

The vessel model uses established relations between actuators, external environmental disturbances (wind), and the motion of the hull through water to describe the forces acting on the hull through the maneuvering model of Fossen [32]. The kinematic model is

$$\dot{\eta} = R(\psi)v \tag{1}$$

where η is the pose vector containing the positions and yaw angle. $R(\psi)$ is the horizontal plane rotation matrix due to the yaw angle ψ. v is the velocity vector in surge, sway, and yaw directions, respectively. Forces due to wind, waves, thrusters, hull friction, and inertia are given in the following equation:

$$M_{\text{RB}}\dot{v} + C_{\text{RB}}(v)v + M_A\dot{v}_r + C_A(v_r)v_r + Dv_r + D_n(v_r)v_r$$
$$= \tau_c + \tau_{wi} + \tau_{wa} \tag{2}$$

where $v_r = v - v_c$ is the relative ship velocity, and $v_c = \begin{bmatrix} u_c & v_c & 0 \end{bmatrix}^T$ is the current velocity. M_{RB} is the rigid body mass matrix, M_A is the added mass matrix, and C_A and C_{RB} are matrices describing the Coriolis/centripetal forces. D and $D_n(v_r)$ are linear and nonlinear damping matrices due to the hull moving through water. τ_c, τ_{wi}, and τ_{wa} are forces on the ship due to thrusters, wind, and wave effects, respectively. At this point, a few simplifications to the vessel model become relevant.

1) *Simplification 1:* Forces due to current are not accounted for in the vessel dynamic model (see (2)). The speed and direction of the current are not measured. Therefore, the velocity of the ship relative to the water, represented by v_r in (2), is not known. v_r is, therefore, substituted by v in (2).

TABLE I
FOUR QUADRANTS OF PROPELLER OPERATION PARAMETERIZED BY RPM AND INFLOW VELOCITY (COURTESY OF [33])

Parameter	1st	2nd	3rd	4th
n	≥ 0	< 0	< 0	≥ 0
V_a	≥ 0	≥ 0	< 0	< 0

2) *Simplification 2:* Forces due to waves, given as τ_{wa} in (2), are not accounted for. This is due to the lack of measurements of the wave state. Besides, ports provide shelter from waves experienced in the open ocean. Therefore, we do not include estimates of forces from waves in the vessel model.

A numerical model of the forces produced by the two main azimuth thrusters was supplied by the thruster manufacturer. It is valid for all four quadrants of operation for the propeller (see Table I) and, thus, covers the key phases of the docking procedure of this study: the initial approach (transit), deceleration (windmilling), and low-speed maneuvering. An introduction to this type of propeller model is given in [33]. With regards to the force produced by the bow tunnel thruster, only the nominal force is estimated through a thruster curve provided by the thruster manufacturer.

To translate the propeller thrust into the 3-D force τ_c, the azimuth angle and distance from the center of gravity of the vessel to each thruster are applied in the following equation:

$$\tau_c = \begin{bmatrix} 0 & c(\alpha_p) & c(\alpha_s) \\ 1 & s(\alpha_p) & s(\alpha_s) \\ l_{tx} & l_{px}s(\alpha_p) & l_{sx}s(\alpha_s) \\ & -l_{py}c(\alpha_p) & -l_{sy}c(\alpha_s) \end{bmatrix} \times \begin{bmatrix} T_{tn} \\ T_{pa} \\ T_{sa} \end{bmatrix} \tag{3}$$

where l_{tx}, l_{px}, and l_{sx} are the distances along the longitudinal axis of the vessel from the vessel center of gravity to the tunnel thruster, port main thruster, and starboard main thruster, respectively. α_p is the azimuth angle of the port main thruster, while α_s is the azimuth angle of the starboard main thruster. The distance from the vessel center of gravity to each of the two main thrusters along the lateral axis of the vessel is given by l_{py} and l_{sy}. $s(\cdot)$ represents the sine function, while $c(\cdot)$ represents the cosine function. Forces produced by each thruster along the propeller axis are given by the variables T_{tn}, T_{pa}, and T_{sa} for the tunnel thruster, port main thruster, and starboard main thruster, respectively. Only lateral force and torque about the up–down axis of the vessel are produced by the bow tunnel thruster.

Wind force is the only external disturbance in which we use a deterministic model to estimate force. This is because the wind (velocity and direction) is the only one of the three environmental states measured. The 3-D force is given in the following equation:

$$\tau_{wi} = \frac{1}{2}\rho_a V_{rw}^2 \begin{bmatrix} C_X(\gamma_{rw})A_{Fw} \\ C_Y(\gamma_{rw})A_{Lw} \\ C_N(\gamma_{rw})A_{Lw}L_{oa} \end{bmatrix} \tag{4}$$

where ρ_a is the density of air, V_{rw} is the relative wind velocity, γ_{rw} is the relative wind angle, and C_X, C_Y, and C_N are wind coefficients specific for the hull/superstructure shape. A_{Fw} and

A_{Lw} are frontal and lateral projected areas, and L_{oa} is the overall length of the ship.

C. Machine Learning Model

Several choices exist when selecting a method for the ML predictor. According to previous work in the domain of ship motion prediction using ML (see Section II-B), SVMs, neural networks (feedforward and recursive), and AR methods are popular choices. We will apply an LSTM network, which has shown outstanding performance in time-series modeling and prediction.

The sequential nature of time-series data related to the motion of ships makes the LSTM a natural choice when searching for a representative model. This network type is specifically designed to store data over an extended period of time, allowing it to capture the relatively slow changes observed in data related to ship motion. Through the use of constant error flow, embodied by the constant error carousels (CECs) in each LSTM block, multiplicative gates that learn when to allow access to the CEC, events, or relations between input- and output data, spaced by a significant time interval, may be approximated [34]. In order to ensure satisfactory performance of the LSTM in predicting future vessel states, hyperparameters need to be set. This is done using the MATLAB software, especially the Bayesian optimization algorithm described in [35]. To limit the search space and, thus, the required computation time, three parameters were included in the search:

1) learning rate;
2) number of LSTM layers;
3) number of blocks per layer.

1) Ensembles: Due to randomness in the weight initialization of the LSTM network, each instantiation of a network with equal hyperparameters will output slightly different predictions faced with the same input data. By averaging the output of several networks, using the same optimized hyperparameters, the prediction error on previously unseen data can be reduced [36].

IV. Experiment

Table III shows the main physical dimensions of the Research Vessel (RV) Gunnerus, an RV owned by the Norwegian University of Science and Technology (NTNU). In terms of propulsors, two azimuth thrusters are mounted at the stern as well as a bow tunnel thruster. The two azimuth thrusters are each driven by a 500-kW electric motor, while the electric motor driving the bow thruster is rated at 200 kW. This yields a cruising speed of about 10 knots.

A. Data

The experiment was conducted based on history data acquired through log files created by a data acquisition system onboard the RV Gunnerus. A one-year time period was selected starting from August 2016 and ending in June 2017. For all variables in the data set, a sampling rate of 1 Hz was observed.

TABLE II
VARIABLES USED IN THIS STUDY AS INPUT TO THE VESSEL MODEL AND LSTM MODEL

Variable name	Unit	Range (train)	Range (test)
North	m	1688/-2703	2267/-769
East	m	1961/-486	1145/-1567
Heading angle	deg	360/0	360/0
Surge speed	knots	11.8/-1.82	11.98/-0.31
Sway speed	knots	1.43/-1.43	1.05/-1.03
Heading rate	deg/s	3.67/-3.43	2.84/-2.81
Roll	deg	2.68/-3.9	2.99/-2.72
Pitch	deg	0.53/-2.09	-0.02/-1.82
Heave	m	0.14/-0.12	0.35/-0.41
Roll rate	deg/s	2.22/-1.97	2.03/-2.17
Pitch rate	deg/s	1.08/-1.28	0.89/-0.69
Heave rate	m/s	0.17/-0.18	0.29/-0.25
Wind direction	deg	360/0	360/0
Wind speed	knots	19/0	15.6/0
Course	deg	360/0	360/0
Total speed	knots	11.8/0	12/0
Port thruster RPM	%	93.96/-67.64	99.19/-51.89
Port thruster angle	deg	121.93/-90.33	156.04/-89.83
Starboard thruster RPM	%	93.95/-67.58	100.08/-56.62
Starboard thruster angle	deg	106.33/-117.33	90.33/-146.44
Tunnel thruster RPM	%	102.1/-99.8	93/-61.2

TABLE III
PHYSICAL PARAMETERS OF THE VESSEL USED IN THE EXPERIMENT

Parameter	Description	Value
m	Mass of vessel	370 t
DWT	Deadweight	107 t
L_{pp}	Length between perpendiculars	28.9 m
Bm	Breadth middle (m)	9.6 m
dm	Draught (m)	2.7 m

In order to isolate successful dockings in the 2016–2017 period, three sensor channels were used. Two Boolean signals originating from the propulsion system, *drive_running* (going from true to false) and *motor_at_zero_speed* (equals true), were applied in combination with a requirement of having a total speed of less than 0.1 m/s. When the docking time instances were successfully determined, 1000 samples prior to these instances were extracted and made up the data set for each docking operation. This interval may contain an initial period of automatic waypoint following control. However, the majority of the time is spent in the manual control mode, in which the ship operator guides the vessel to its docking location. Twenty-one sensor channels related to the motion of the vessel were sampled (see the first column of Table II), leading to a 1000×21 matrix of measurements per operation, spanning 15 locations along the west coast of Norway (see Fig. 3).

Table II gives all the input variables for the hybrid predictor used in this study. Ranges are given as maximum and minimum values observed in the time series of each variable during 88 separate docking operations. Of these, the first 68 were used for training, and the last 20 were kept for testing purposes. The unit deg is short for degrees. To get a clearer sense of the nature of each variable, and the extreme values observed in
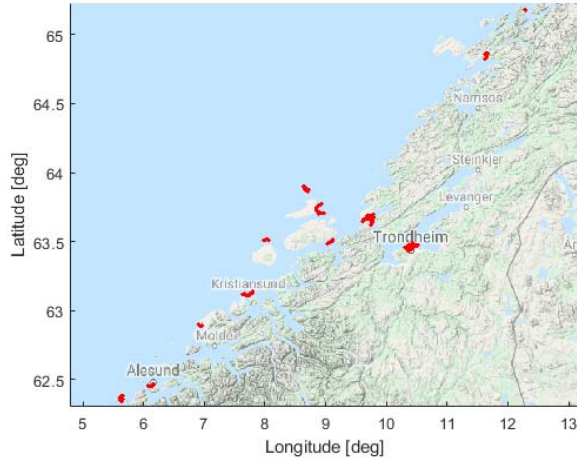
Fig. 3. Various docking locations of the RV Gunnerus along the west coast of Norway.

(a) Training

(b) Testing

Fig. 4. North–east path taken by the RV Gunnerus for all docking operations used in this study.

the training data compared with the testing data, the max/min values are given in columns 3 and 4 of Table II.

Further processing of the position of the ship was made in order to generalize the position coordinates across docking locations. A conversion from the position given as latitude and longitude in the earth-centered, earth-fixed (ECEF) frame to the local north–east–down (NED) frame in meters, was performed for convenience. The ECEF position recorded at the docking time instance was used as the origin for the NED coordinates of each docking operation. Fig. 4(a) and (b) shows the path taken by the vessel toward the docking location at coordinates (0, 0) m. The former shows all paths included as training instances for the ML algorithms, while the latter shows the test instances.

### B. Prediction for One Docking Approach

As mentioned in Section IV-A, training data for the ML predictor consisted of 68 individual docking operations. First running the vessel model predictor on each time instance (1000 instances per docking operation), predicting 30 s ahead of real time, made it possible to generate an error signal by subtracting the vessel model position prediction from the actual position of the vessel. Thereby, the training targets, one vector with a 30-s prediction horizon per sampling instance, for the supervised training of the LSTM networks were created. Fig. 5 shows the accuracy of the predictions in terms of average distance errors, calculated by (5), in the north–east plane for each docking operation in the training data

$$\bar{y}_{\text{err},i} = \left(\sum_{j=1}^{M} \sqrt{(N_{ij} - \hat{N}_{ij})^2 + (E_{ij} - \hat{E}_{ij})^2} \right) / M \quad (5)$$

where $\bar{y}_{\text{err}}$ is the mean distance error between the predicted and the true position of the ship in the prediction interval, M is the number of samples per docking operation, and $i \in [1, 30]$ is the index of the prediction horizon, t_h. N and E represent the true north and east positions, respectively, while $\hat{N}$ and $\hat{E}$ are the predicted north and east positions.
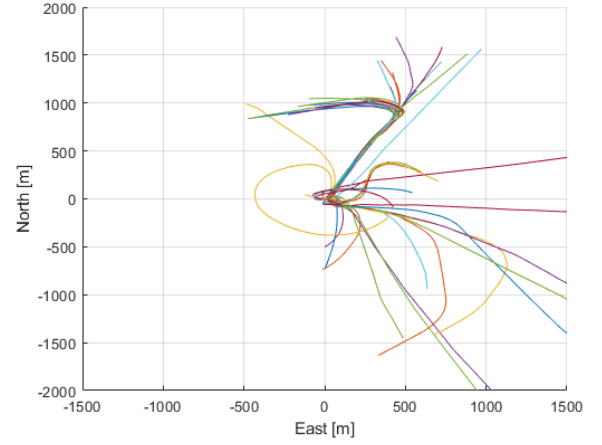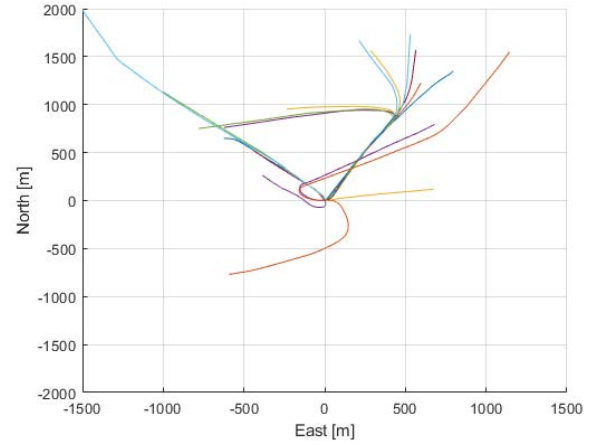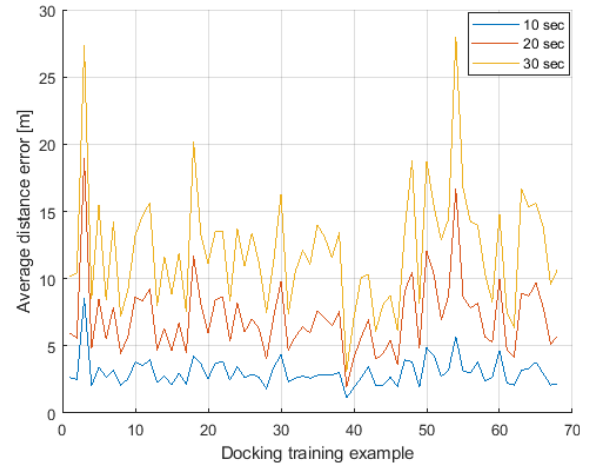

Fig. 5. Average distance between the true position and the position estimated by the vessel model at 10-, 20-, and 30-s prediction horizons on the training examples.

Given input data according to Section III-B at a certain time instance, the vessel model predictor iteratively predicts the position of the vessel 30 s ahead. In parallel, the ML predictor offers predictions of the position prediction error
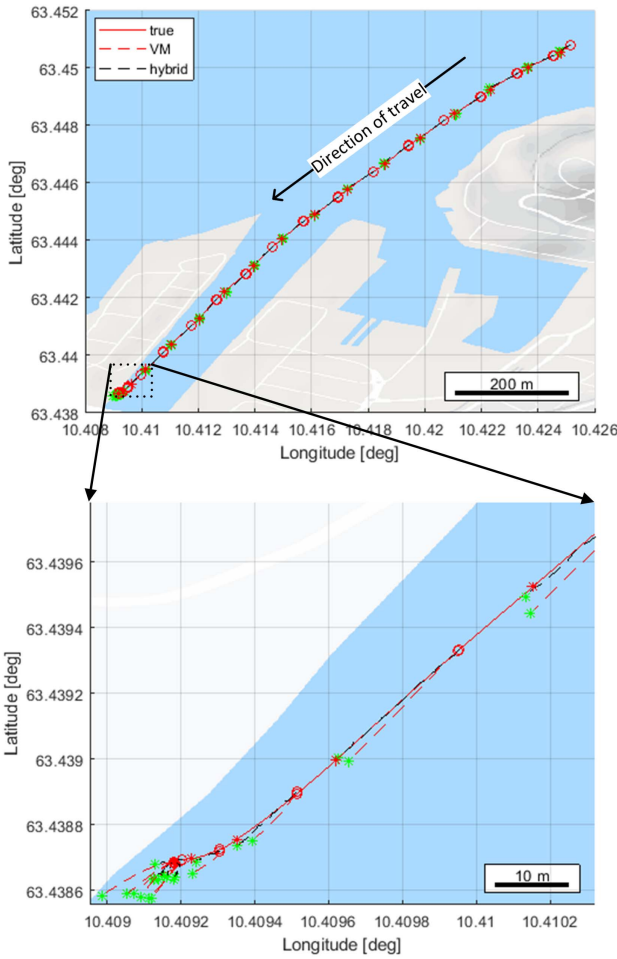
Fig. 6. Prediction of ship position in the horizontal plane in the port of Trondheim, Norway.
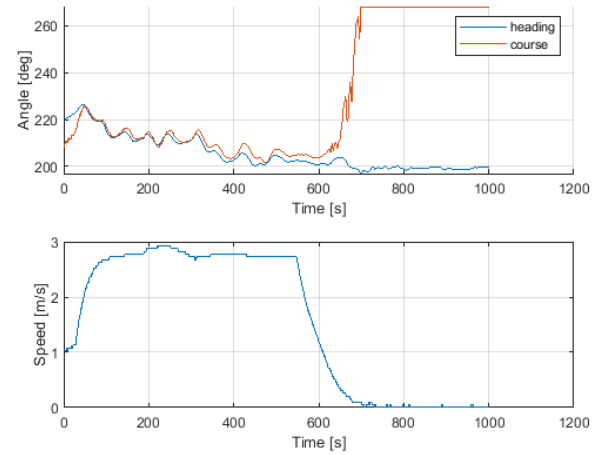

Fig. 7. Top plot shows the heading and course angle of the ship while docking in Trondheim, while the bottom plot shows the ship speed.
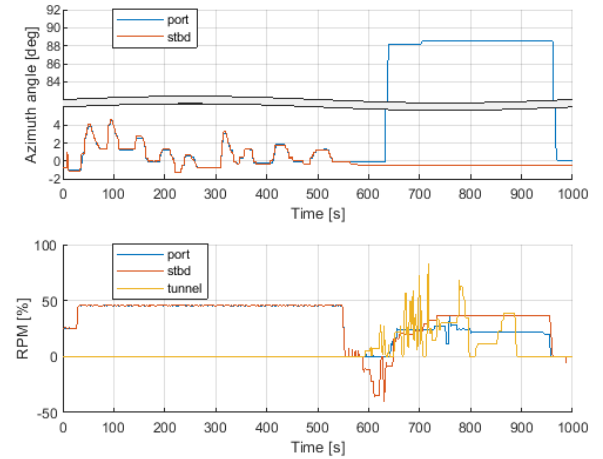

Fig. 8. Top plot shows the rotation angle of the main thrusters, while the bottom plot shows the RPM percentage of all three thrusters.

made by the vessel model predictor. The sum of these two 30-element vectors constitutes the end result of the prediction approach: a set of coordinates given for future time instances in the north–east plane.

This is visualized in the plots of Fig. 6, which shows the actual track of the docking approach and predictions made every 45 s. The red circle marks the start of each prediction, while the green star marks the end for both the hybrid predictor and the vessel model predictor. The red star shows the true position at the prediction interval end. If the red and green stars overlap, the position is predicted perfectly at 30 s ahead of real time. As the area between the true track of the vessel (red solid line) and the hybrid prediction vector (black dashed line) is smaller compared with the vessel model prediction vector, the hybrid predictor has better position prediction accuracy. This is also evident from the prediction error for the prediction horizon end (distance between each green star and the adjacent red star).

Both the vessel model predictions and the hybrid model predictions diverge from the true position close to the origin. This is attributed to the use of thrusters to temporarily push the vessel against the dock while preparing the mooring ropes. Figs. 7 and 8 show that while the speed of the vessel

approaches zero at $t \approx 700$ s, indicating that the vessel has docked, the thrusters are still producing thrust. In the same time period, the course angle of Fig. 7 is invalid due to zero speed. At $t \approx 630$ s, the top figure in Fig. 8 shows the port thruster being rotated. This is to push the vessel toward the dock with the starboard side facing the dock.

The top figure in Fig. 7 shows the plots of the course angle against the heading angle. For the final approach to the Trondheim docking location, the course and heading angle deviate by several degrees in the time period 300–500 s. This is due to the dock being located in the outlet of the Nidelva river, and the water flowing toward the sea induces a force on the hull. The effect on the vessel model prediction was a steady error of approximately 5 m in the north–east plane during this time period.

C. Average Performance

Fig. 9 shows the performance of the hybrid predictor and the vessel model predictor. The number of samples for the averaging of the position prediction at future times $t_h = [1, 30]$ s includes the entire 1000 s prior to completing the
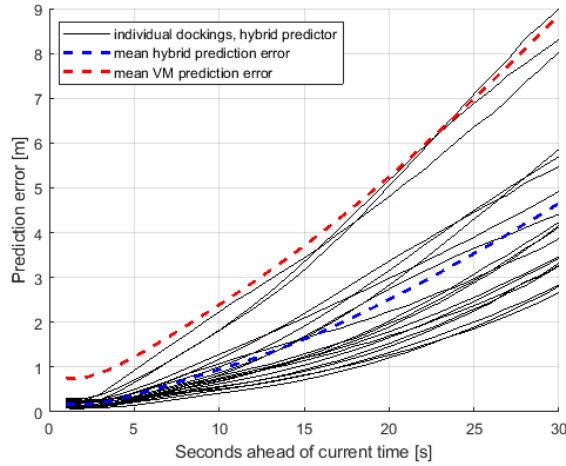
Fig. 9. Average position prediction error of the vessel model predictor by itself (red dashed line) and the hybrid predictor (dashed blue line) over the 20 test sets and the prediction horizon (1–30 s). The black solid lines represent the average position prediction error of the 20 individual docking operations included in the test set for the hybrid predictor.

TABLE IV
AVERAGE POSITION PREDICTION ERROR MADE BY
THE VESSEL MODEL PREDICTOR

t_h [s]	Training error [m]	Testing error [m]
10	3.04	2.34
20	7.11	5.23
30	12.11	8.85

docking operation. Typically, this involves a short initial period of transit speed, followed by deceleration to a low-speed approach and finally gliding/decelerating toward close-to-zero speeds. This final period usually involves the application of the bow tunnel thruster (see the bottom figure in Fig. 8). Both the vessel model predictor and the LSTM model predictor can introduce prediction error to the overall hybrid predictor. However, the main sources of error come from the vessel model and are due to the following reasons.

1) The vessel model predictor does not account for forces induced by current as they are not measured.
2) Change in the control commands input by the vessel operator is unknown within each prediction interval and therefore the initial value is applied.

The LSTM predictor assumes a portion of this error, which results in an improved overall position prediction, reducing the average prediction error at $t_h = 30$ s by almost half. While there are three docking operations that exhibit close to the same accuracy as the vessel model prediction average (three black lines close to the red dashed line of Fig. 9), two of them are at a docking location not covered in the training data set. The third line is generated by predictions carried out while docking in a port, which is covered only once in the training data set, and in an irregular fashion as well. It is irregular in the sense that the vessel did not follow the usual pattern of deceleration but moved toward the dock in lurches. The remaining black lines in Fig. 9 depict the prediction errors incurred while docking at more frequently visited docking locations.

Due to the nature of data-based models, where the training data dictate the performance of the trained model, the more repetitions of docking at a certain port will lead to the hybrid predictor providing better predictions at this location. For the application described in this article, if the trained hybrid predictor was applied while docking the ship at a port for the first time, it would perform worse than if it docked at its home

port of Trondheim. However, by including the vessel model predictor, which provides a deterministic evaluation of the position prediction, along with facilities in the LSTM predictor to maintain its generalization abilities (regularization, early stopping training and dropout layer), an increase in position prediction accuracy is seen compared with the predictions made by the vessel model predictor alone. Downsides to this hybrid predictor include the requirement of having both a sufficient amount of data for training of the data-based model as well as the parameters of the dynamic model described in Section III-B.

The second column of Table IV displays the averages of the values seen for $t_h = [10, 20, 30]$ s in Fig. 5. A lower average prediction error is observed for the testing data relative to the training data. This is due to the diversity of docking locations contained in each set. Out of 15 docking locations, four are represented in the test set, while 14 are represented in the training set. Thus, as every docking location has its own set of challenges with respect to geographical layout and environmental conditions, the ship operator needs to adapt his or her docking strategy. This results in a larger spread in terms of thruster commands, which, in turn, affects the prediction accuracy of the vessel model.

V. CONCLUSION

Predicting the motion of a ship is complex. As a way to reduce the uncertainty of the position predictor performance, predictions originating from the vessel dynamic model were combined with a data-based predictor. The latter was implemented using the LSTM neural network methodology. This resulted in a hybrid predictor, where the data-based LSTM corrected the predictions made by the vessel model. A substantial increase in average accuracy was observed throughout the prediction interval. At the maximum prediction horizon of 30 s, the average distance error in the position predictions was reduced by about 4 m, from 8.9 (vessel model) to 4.7 m (hybrid model). Although the black-box nature of the LSTM does not allow for direct insight into what causes the vessel model predictions to deviate, it compensates for the deviations, producing more accurate predictions when both predictors are combined.

This study applies prediction solely to provide additional information for the ship operator while docking. Utilizing the proposed hybrid position prediction as input to an automatic motion controller could improve the efficiency and accuracy of autonomous docking operations. Providing a hybrid predictor that meets the two-sided goal of maintaining the stability of the cascaded predictor-controller system, as well as to accurately predict the vessel dynamics, would be a key challenge.

Along with the inclusion of wind predictions into the hybrid predictor, this constitutes the direction of future work.

REFERENCES

[1] X. Yang, "Displacement motion prediction of a landing deck for recovery operations of rotary UAVs," *Int. J. Control, Autom. Syst.*, vol. 11, no. 1, pp. 58–64, Feb. 2013.

[2] P. From, J. Gravdahl, and P. Abbeel, "On the influence of ship motion prediction accuracy on motion planning and control of robotic manipulators on seaborne platforms," in *Proc. Int. Conf. Robot. Autom.*, May 2010, pp. 5281–5288.

[3] S. Küchler, T. Mahl, J. Neupert, K. Schneider, and O. Sawodny, "Active control for an offshore crane using prediction of the vessel's motion," *IEEE/ASME Trans. Mechatronics*, vol. 16, no. 2, pp. 297–309, Apr. 2011.

[4] T. Praczyk, "Using evolutionary neural networks to predict spatial orientation of a ship," *Neurocomputing*, vol. 166, pp. 229–243, Oct. 2015.

[5] Y. Shuai *et al.*, "An efficient neural-network based approach to automatic ship docking," *Ocean Eng.*, vol. 191, Nov. 2019, Art. no. 106514.

[6] L. P. Perera, "Navigation vector based ship maneuvering prediction," *Ocean Eng.*, vol. 138, pp. 151–160, Jul. 2017.

[7] M. Triantafyllou, M. Bodson, and M. Athans, "Real time estimation of ship motions using Kalman filtering techniques," *IEEE J. Ocean. Eng.*, vol. 8, no. 1, pp. 9–20, Jan. 1983.

[8] S. Sutulo, L. Moreira, and C. G. Soares, "Mathematical models for ship path prediction in manoeuvring simulation systems," *Ocean Eng.*, vol. 29, no. 1, pp. 1–19, Jan. 2002.

[9] M. M. Sidar and B. F. Doolin, "On the feasibility of real-time prediction of aircraft carrier motion at sea," *IEEE Trans. Autom. Control*, vol. AC-28, no. 3, pp. 350–356, Mar. 1983.

[10] U. D. Nielsen, A. H. Brodtkorb, and J. J. Jensen, "Response predictions using the observed autocorrelation function," *Mar. Struct.*, vol. 58, pp. 31–52, Mar. 2018.

[11] L. P. Perera and C. G. Soares, "Ocean vessel trajectory estimation and prediction based on extended Kalman filter," in *Proc. 2nd Int. Conf. Adapt. Self-Adapt. Syst. Appl.*, 2010, pp. 14–20.

[12] L. P. Perera, P. Oliveira, and C. G. Soares, "Maritime traffic monitoring based on vessel detection, tracking, state estimation, and trajectory prediction," *IEEE Trans. Intell. Transp. Syst.*, vol. 13, no. 3, pp. 1188–1200, Sep. 2012.

[13] Y.-M. Yin, H.-Y. Cui, M. Hong, and D.-Y. Zhao, "Prediction of the vertical vibration of ship hull based on grey relational analysis and SVM method," *J. Mar. Sci. Technol.*, vol. 20, no. 3, pp. 467–474, Sep. 2015.

[14] M.-W. Li, J. Geng, D.-F. Han, and T.-J. Zheng, "Ship motion prediction using dynamic seasonal RvSVR with phase space reconstruction and the chaos adaptive efficient FOA," *Neurocomputing*, vol. 174, pp. 661–680, Jan. 2016.

[15] W. Zhang and Z. Liu, "Real-time ship motion prediction based on time delay wavelet neural network," *J. Appl. Math.*, vol. 2014, pp. 1–7, Jan. 2014.

[16] Z. Peng, J. Wang, and D. Wang, "Distributed containment maneuvering of multiple marine vessels via neurodynamics-based output feedback," *IEEE Trans. Ind. Electron.*, vol. 64, no. 5, pp. 3831–3839, May 2017.

[17] Z. Peng, J. Wang, and D. Wang, "Distributed maneuvering of autonomous surface vehicles based on neurodynamic optimization and fuzzy approximation," *IEEE Trans. Control Syst. Technol.*, vol. 26, no. 3, pp. 1083–1090, May 2018.

[18] J. Yin, W. Zhang, T. Li, and J. Hu, "Modified minimal resource allocating network for ship motion predictive control," in *Proc. Int. Conf. Intell. Control Inf. Process.*, Aug. 2010, pp. 231–235.

[19] J.-C. Yin, Z.-J. Zou, and F. Xu, "On-line prediction of ship roll motion during maneuvering using sequential learning RBF neuralnetworks," *Ocean Eng.*, vol. 61, pp. 139–147, Mar. 2013.

[20] R. Skulstad, G. Li, T. I. Fossen, B. Vik, and H. Zhang, "Dead reckoning of dynamically positioned ships: Using an efficient recurrent neural network," *IEEE Robot. Autom. Mag.*, vol. 26, no. 3, pp. 39–51, Sep. 2019.

[21] Q. Xu, X. Li, and C.-Y. Chan, "Enhancing localization accuracy of MEMS-INS/GPS/in-vehicle sensors integration during GPS outages," *IEEE Trans. Instrum. Meas.*, vol. 67, no. 8, pp. 1–13, Mar. 2018.

[22] L. Chen and J. Fang, "A hybrid prediction method for bridging GPS outages in high-precision POS application," *IEEE Trans. Instrum. Meas.*, vol. 63, no. 6, pp. 1656–1665, Jun. 2014.

[23] J. Ma, T. Li, and G. Li, "Comparison of representative method for time series prediction," in *Proc. Int. Conf. Mechatronics Autom.*, Jun. 2006, pp. 2448–2453.

[24] W.-Y. Duan, L.-M. Huang, Y. Han, and R. Wang, "IRF–AR model for short-term prediction of ship motion," in *Proc. 25th Int. Ocean Polar Eng. Conf.*, Jul. 2015, pp. 59–66.

[25] Z. Xiao, L. Ponnambalam, X. Fu, and W. Zhang, "Maritime traffic probabilistic forecasting based on vessels' waterway patterns and motion behaviors," *IEEE Trans. Intell. Transp. Syst.*, vol. 18, no. 11, pp. 3122–3134, Nov. 2017.

[26] S. Gan, S. Liang, K. Li, J. Deng, and T. Cheng, "Long-term ship speed prediction for intelligent traffic signaling," *IEEE Trans. Intell. Transp. Syst.*, vol. 18, no. 1, pp. 82–91, Jan. 2017.

[27] J. M. Giron-Sierra and S. Esteban, "The problem of quiescent period prediction for ships: A review," *IFAC Proc. Volumes*, vol. 43, no. 20, pp. 307–312, 2010.

[28] J. G. Kusters, K. L. Cockrell, B. S. H. Connell, J. P. Rudzinsky, and V. J. Vinciullo, "FutureWaves: A real-time ship motion forecasting system employing advanced wave-sensing radar," in *Proc. OCEANS MTS/IEEE Monterey*, Sep. 2016, pp. 1–9.

[29] E. Soares, P. Costa, B. Costa, and D. Leite, "Ensemble of evolving data clouds and fuzzy models for weather time series prediction," *Appl. Soft Comput.*, vol. 64, pp. 445–453, Mar. 2018.

[30] N. Sapankevych and R. Sankar, "Time series prediction using support vector machines: A survey," *IEEE Comput. Intell. Mag.*, vol. 4, no. 2, pp. 24–38, May 2009.

[31] S. Lefèvre, D. Vasquez, and C. Laugier, "A survey on motion prediction and risk assessment for intelligent vehicles," *Robomech J.*, vol. 1, no. 1, pp. 1–14, Dec. 2014.

[32] T. I. Fossen, *Handbook of Marine Craft Hydrodynamics and Motion Control*. Hoboken, NJ, USA: Wiley, 2011.

[33] O. N. Smogeli, "Control of marine propellers: From normal to extreme conditions," Ph.D. dissertation, Dept. Mar. Technol., Norwegian Univ. Sci. Technol., Trondheim, Norway, 2006.

[34] J. Schmidhuber, "Deep learning in neural networks: An overview," *Neural Netw.*, vol. 61, pp. 85–117, Jan. 2015.

[35] J. Snoek, H. Larochelle, and R. Adams, "Practical Bayesian optimization of machine learning algorithms," in *Proc. Adv. Neural Inf. Process. Syst.*, 2012, pp. 2951–2959.

[36] S. G. Soares and R. Araújo, "An adaptive ensemble of on-line extreme learning machines with variable forgetting factor for dynamic system prediction," *Neurocomputing*, vol. 171, pp. 693–707, Jan. 2016.

Robert Skulstad received the M.Sc. degree in engineering cybernetics from the Norwegian University of Science and Technology (NTNU), Trondheim, Norway, in 2014. He is currently pursuing the Ph.D. degree with the Intelligent Systems Laboratory, Department of Ocean Operations and Civil Engineering, NTNU, Ålesund, Norway.

His research interests include ship motion prediction, machine learning, and ship motion control.

Guoyuan Li (Senior Member, IEEE) received the Ph.D. degree in computer science from the Department of Informatics, Institute of Technical Aspects of Multimodal Systems, University of Hamburg, Hamburg, Germany, in 2013.

In 2014, he joined the Department of Ocean Operations and Civil Engineering, Intelligent Systems Laboratory, Norwegian University of Science and Technology, Ålesund, Norway. In 2018, he became an Associate Professor of ship intelligence. He has published more than 60 articles in the areas of his research interests, including modeling and simulation of ship motion, autonomous navigation, intelligent control, optimization algorithms, and locomotion control of bioinspired robots.

Thor I. Fossen (Fellow, IEEE) received the M.Sc. degree in marine technology and the Ph.D. degree in engineering cybernetics from the Norwegian University of Science and Technology (NTNU), Trondheim, Norway, in 1987 and 1991, respectively.

He is one of the co-founders and the former Vice President of the Research and Development of Marine Cybernetics AS, Trondheim, which was acquired by DNV GL, Oslo, Norway, in 2012. He was the Co-Founder of SCOUT Drone Inspection AS, Trondheim, in 2017. He is currently a Professor of guidance, navigation and control and the Co-Director of the NTNU Centre for Autonomous Marine Operations and Systems. He is also a Naval Architect and a Cyberneticist. He has authored six textbooks. His research interests include guidance systems, inertial navigation systems, nonlinear control and observer theory, vehicle dynamics, hydrodynamics, autopilots, and unmanned vehicles.

Dr. Fossen received the Automatica Prize Paper Award in 2002 and the Arch T. Colwell Merit Award in 2008 at the SAE World Congress. He has been elected to the Norwegian Academy of Technological Sciences in 1998.

Bjørnar Vik received the M.Sc. and Ph.D. degrees in engineering cybernetics from the Norwegian University of Science and Technology (NTNU), Trondheim, Norway, in 1994 and 2000, respectively.

From 2000 to 2003, he held a post-doctoral position at NTNU. He joined Marine Cybernetics AS, Trondheim, in 2004. From 2004 to 2014, he worked with Marine Cybernetics, developing simulators and test methods for hardware-in-the-loop testing of control systems, and an Adjunct Associate Professor with NTNU. Since 2014, he has been working at Rolls-Royce Marine and Kongsberg Maritime, Ålesund, Norway, where he is currently a Principal Engineer of simulation and control.

Houxiang Zhang (Senior Member, IEEE) received the M.Sc. and Ph.D. degrees in mechanical and electronic engineering from the Robotics Institute, Beihang University, Beijing, China, in 2000 and 2003, respectively, and the Habilitation degree in informatics from the University of Hamburg, Hamburg, Germany, in February 2011.

In 2004, he worked as a Post-Doctoral Fellow and a Senior Researcher with the Department of Informatics, Faculty of Mathematics, Informatics and Natural Sciences, Institute of Technical Aspects of Multimodal Systems (TAMS), University of Hamburg. In April 2011, he joined Norwegian University of Science and Technology (NTNU), Ålesund, Norway, where he is currently a Professor of mechatronics. He has been engaged in two main research areas, including biological locomotion control, and digitalization and virtual prototyping in demanding marine operation. He has applied for and coordinated more than 30 projects supported by the Norwegian Research Council (NFR), the German Research Council (DFG), EU, and industry. In these areas, he has published over 200 journal and conference papers as an author or a coauthor.

Dr. Zhang has received four best paper awards and four finalist awards for the best conference paper at the International Conference on Robotics and Automation. He has been elected to the Norwegian Academy of Technological Sciences in 2019.